Friction torque in four-point contact slewing bearings: applicability and limitations of current analytical formulations

Iker Heras [a,]$, Josu Aguirrebeitia [a], Mikel Abasolo [a], Jon Plaza [b]

[a] Department of Mechanical Engineering, ETSI-BILBAO, University of the Basque Country, Alameda de Urquijo, s/n, 48013 Bilbao, Spain
[b] Simulation Tools Development Department, Cikatek S.Coop., 48710 Berriatua, Spain

$ Corresponding author.
E-mail addresses: iker.heras@ehu.eus (I. Heras), josu.aguirrebeitia@ehu.eus (J. Aguirrebeitia), mikel.abasolo@ehu.eus (M. Abasolo), j.plaza.gonzalez@gmail.com (J. Plaza)

ABSTRACT

The friction torque is a key parameter in the design of slewing bearings. The most challenging issue in its calculation resides in the modelling of rolling element contact mechanics. In this manuscript two models for the friction torque calculation are compared: a Finite Element model and the analytical model proposed by Leblanc and Nelias. The last one assumes that full sliding occurs in the ball-raceway contact, which is demonstrated to be an appropriate simplification for many cases, but not for applications where large tilting moments are involved. The objective of this work is to determine the field of application of the analytical model, highlighting its limitations and therefore justifying further research to implement more complex formulations for the contact simulation.

KEYWORDS
slewing bearing; four-point contact; friction torque; ball-raceway contact

1. INTRODUCTION

Slewing bearings are used in a wide variety of applications. Their capacity to face large tilting moments and loads in any axial or radial directions is essential for orientation purposes in tower cranes, vertical lathe tables or radio telescopes, among others. Besides, slewing bearings are used for yaw and pitch rotations in wind turbines and the orientation of the solar trackers. For that reason, the renewable energy industry is demanding a deeper knowledge about these elements. As it is known, the tendency in renewable energy technologies is to increase the dimensions in order to obtain the maximum possible energy, which increases the involved loads as well. The more demanding work conditions, combined with the need to optimize the machines to make them competitive in the energy market, constitute a demand for a better understanding of the involved components.

In this context, the torque required to rotate the orientation system is a very relevant parameter. An actuation system is needed to apply this torque, so estimating its value is mandatory. In order to correctly estimate the friction torque, the load distribution among the balls (due to acting loads) must be determined as a first step. This was studied by Zupan and Prebil for single row four-point contact slewing bearings, which proposed [1] and experimentally validated [2] a method to study the effect of geometrical parameters and the stiffness of the supporting structures in the load carrying capacity. Later, Amasorrain et al. discussed an analytical model for determining the ball loads where only the stiffness of the contact between the rolling elements and raceways was taken into account [3], dismissing the effect of ring deformation. With the same assumption, Aguirrebeitia et al. developed a procedure to determine the acceptance surface in the load space [4–6], considering ball preload and contact angle variation. Olave et al. used superelement techniques to implement the elastic behaviour of the rings and the adjacent structures in the load distribution problem [7] to Amasorrain's model, proving that this fact can affect significantly the results. The superelement techniques were also used by Plaza et al. for wind turbine applications [8], significantly reducing the computational cost for a particular pitch bearing assembly, without accuracy loss. Another key aspect is the raceway manufacturing errors, whose influence on the ball load distribution was studied by Aithal et al. [9]. In this research line, the authors proposed an analytical procedure to calculate the ball-raceway interferences due to manufacturing errors [10], further studying its effect on the friction torque.

On the other hand, for the friction torque calculation, the behaviour of the ball-raceway contact must be characterized. In this sense, Jones solved ball kinematics for angular contact ball bearings by imposing the equilibrium conditions in the bearing, assuming full sliding in the ball-raceway contact [11]. This work was

generalized for four-point contact bearings by Leblanc and Nelias [12,13]. Later, several methods where proposed by Lacroix et al. to account for the flexibility of the rings [14]. All of these works included inertial effects. Nevertheless, in slewing bearings for orientation purposes, the operational velocities are usually low and thus inertial effects are negligible. Consequently, the load distribution problem and the kinematics can be decoupled and therefore solved separately, which simplifies the solution of the equation system. This way, Joshi et al. particularized the problem for slow speed applications and formulated the friction torque calculation [15].

Like in Jones' work, state of the art models for four-point contact bearings assume full sliding in the contact. However, in slewing bearings for wind turbines or solar trackers, there are only two points in contact in regular working conditions because of the large tilting moments (Figure 1a), so balls roll like in a typical angular contact bearing, and consequently stick regions will exist in the contact area according to the Heathcote slip [16]. Due to the low velocities, the area of the stick regions can be significant in the contact ellipse (Figure 1b), contravening the assumption of full sliding made by Jones and Leblanc and Nelias. Thus, it is expected that the described models may not be accurate enough for the friction torque calculation in wind or solar slewing bearings. In this sense, the aim of this work is to define the field of application and therefore the limitations of Leblanc's model [12,13] by Finite Element (FE) analyses using the model previously developed by the authors [17]. Besides, a sensitivity analysis of different parameters in the stick region has been conducted. The results demonstrate that not considering stick regions may lead to inaccurate results when estimating the friction torque in slewing bearings with large tilting moments. Therefore, the need for more complex contact formulations, such as the ones proposed by Kalker [18], is evidenced.

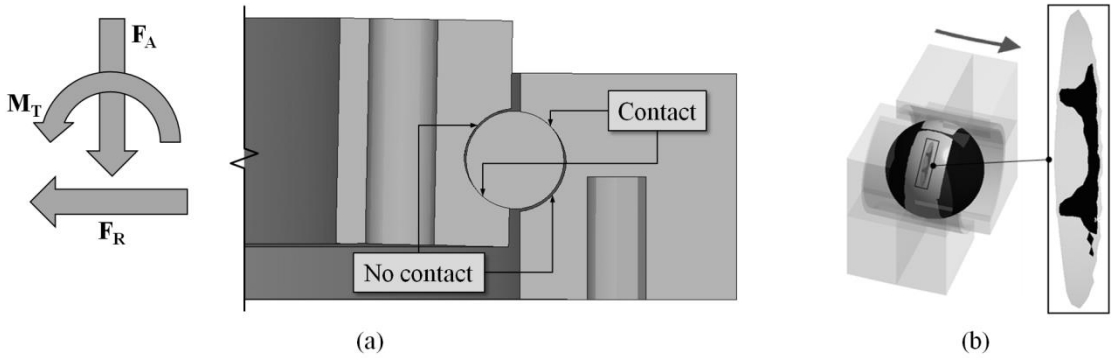

Figure 1. Two contact point case: (a) deformed shape of a bearing under applied loads; (b) stick region in a two contact point case.

2. FRICTION TORQUE CALCULATION MODELS

As explained in the previous section, for slewing bearings the load distribution problem and the kinematics can be decoupled. In this case, Figure 2 shows the flowchart for the calculation of the friction torque, where the different simulation techniques for each problem are presented. In this work, friction torque is computed from the FE model and the analytical model proposed by Leblanc and Nelias. For both models, the ball loads (Q) and contact angles (α) used for torque calculation are the same (as it will be explained later), so a direct comparison is made between analytical and FE results.

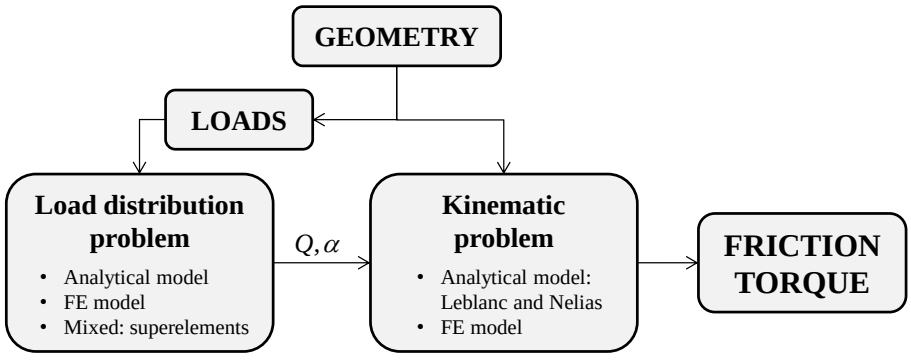

Figure 2. General schema for the friction torque calculation

2.1. Finite Element model

The FE model was previously developed by the authors [17] in ANSYS® Workbench. It is a fully parametric model, where only one ball is considered, with the corresponding portions of inner and outer rings. In this study, ball-raceway interferences (δ) for given contact angle (α) are directly applied instead of external loads, as in [10]; in order to apply these interferences, an offset is introduced to the ball-raceway contact in the first load step, as done by Aithal et al. [9]. Then, in a second step, the inner ring is rotated while the outer one remains fixed. The rotation is gradually introduced, so the kinematics and the contact phenomena can be tracked over time. This study focuses on the local behaviour of the contact and not on the global response of the bearing. In this sense, no deformation of the outer surfaces of the rings is allowed (Figure 3a); this condition simulates rigid rings, while the contact elasticity is suitably simulated.

The main complexity of the model lies on the correct formulation of the ball-raceway contact. In this sense, the Augmented Lagrange formulation is used, while the stiffness of the contact is updated in each iteration, allowing a maximum mesh penetration of 0.1μm. A regular high order hexahedron based mesh is used for the contact region (Figure 3b), which has been adequately refined (Figure 3c) in comparison with the model from [10] in order to obtain detailed contact results. Thus, a FE model with $3.6 \cdot 10^6$ degrees of freedom has been used, with a computational cost of approximately 10 hours per each analysis in a high performance work station. Taking into account the number of calculations needed for the study presented in this manuscript and the available calculation capacity, a more refined model was unapproachable in terms of computational cost. The model shows no convergence problems with the described contact formulation and mesh.

Several outputs are obtained from the analysis. From the first load step, normal loads at different contact points (Q) are computed. From the second load step, the kinematics of the bearing, the contact status (which shows the stick and slip regions of the contact ellipse) and shear stress field and finally the friction torque are reported. Regarding shear stresses, ANSYS® Workbench only plots the modulus but not the direction, so an APDL macro was developed to export these results and visualize them in Matlab®.

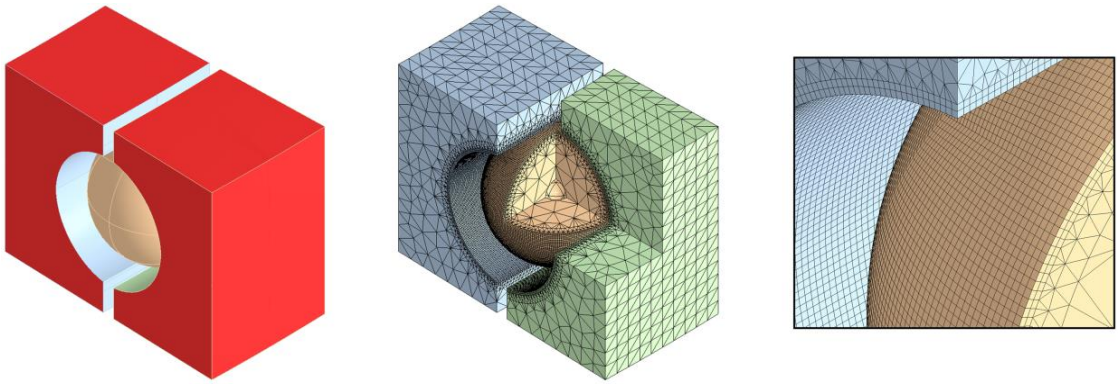

Figure 3. FE model: (a) rigid faces; (b) mesh; (c) detailed view.

2.2. Analytical model

The particularization of the analytical model of Leblanc and Nelias for the case of slow speeds proposed by Joshi et al. [15] was programmed in Matlab®. Using the ball loads (Q) obtained from the FE model as explained in the previous section, the analytical model solves the kinematics and calculates the contact shear stresses and the friction torque of the bearing. As mentioned, the purpose of this work is to compare analytical and FE results in order to outline the applicability and limitations of the analytical model.

Four parameters must be calculated in the kinematic problem: the angular velocities of the outer ring (ω_o), inner ring (ω_i) and ball (ω_B) for a viewer located in the centre of the ball, and finally the angle β that defines the direction of ω_B [12]. Contact shear stress field and friction torque depend on the relation between ω_o, ω_i, ω_B and β; however, since inertial effects are negligible in slewing bearings, these results do not depend on the rotation speed. Thus, one of the four unknown parameters must be an input for the model, while the other ones will be output parameters; in this work, ω_i was taken as the input parameter (obviously, contact shear stress field and friction torque results were found to be the same regardless of the magnitude of ω_i).

The equilibrium conditions to solve the kinematics are formulated in [15]. An accurate initial guess of parameters ω_o, ω_i, ω_B and β is necessary to ensure the convergence. In this work, the following expressions are proposed from the assumption that ball-raceway slip is equally divided among the contacting points:

$$\frac{\omega_o}{\omega_i} = -\frac{\frac{D_{pw}}{D_w} - cos\left(\frac{\alpha'_1 + \alpha'_2}{2}\right)}{\frac{D_{pw}}{D_w} + cos\left(\frac{\alpha'_1 + \alpha'_2}{2}\right)} \tag{1}$$

$$\frac{\omega_B}{\omega_i} = \frac{\frac{D_{pw}}{D_w} - cos\left(\frac{\alpha'_1 + \alpha'_2}{2}\right)}{cos\left(\phi\frac{\alpha'_1 + \alpha'_2}{2}\right)} \tag{2}$$

$$\beta = \pi + \frac{\alpha'_2 - \alpha'_1}{2} \tag{3}$$

Where D_{pw} is the mean diameter of the bearing, D_w is the ball diameter and α'_1, α'_2 and ϕ are given by Table 1. In the table, α_1 is the contact angle for contact diagonal 1, defined by contact points (CP) 1 and 3 (see Figure 4), whereas α_2 is the contact angle for contact diagonal 2, defined by contact points 2 and 4. The initial guess from equations (1-3) was found to be very close to the final results for two-point contact cases (only one contact diagonal) and for four-point contact cases if both diagonals are equally loaded. In the first situation, the ball is rolling; in the second situation, the ball is spinning. When two diagonals are asymmetrically loaded, the kinematics will be close to one of these situations, depending on the loading ratio between both diagonals.

Contact diagonal	α'_1	α'_2	ϕ
1 (CP1-CP3)	$2\alpha_1$	0	0
2 (CP2-CP4)	0	$2\alpha_2$	0
1 and 2	α_1	α_2	1

Table 1. Values of the parameters for the initial guess.

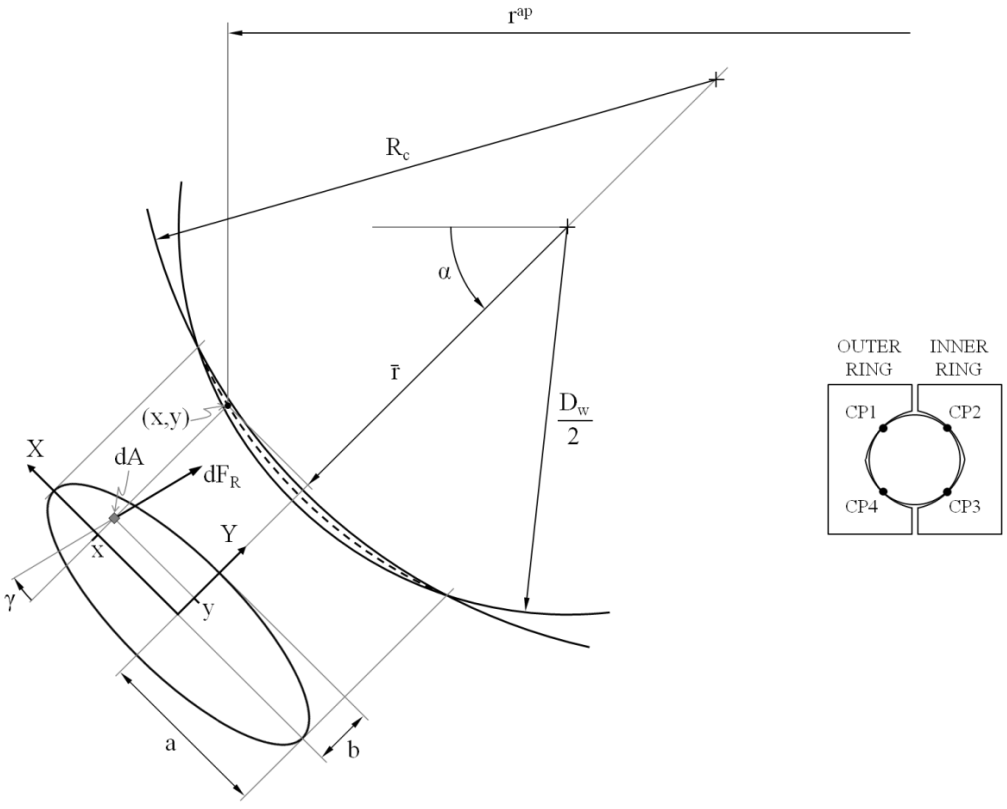

Figure 4. Contact ellipse, geometric parameters and contact numbering.

For the calculation of the friction torque, a different approach from that proposed by Joshi et al. was used. While in [15] the friction torque was computed from the resultant forces and moments applied in the effective rolling radii, the results in the present work were obtained directly integrating the circumferential component of the friction force (F_R) in the contact ellipse. Thus, the friction torque in the outer and inner ring (which will have the same value but with opposite sign) are:

$$M_f = \sum_i \frac{3Q_i\mu}{2\pi} \int_0^{2\pi} \int_0^1 \rho\sqrt{1-\rho^2}\, cos\gamma\, r_i^{ap}\, d\rho\, d\theta \quad \text{where} \quad \begin{cases} i = 1{,}4 & \text{for the outer ring} \\ i = 2{,}3 & \text{for the inner ring} \end{cases} \tag{4}$$

Where the radius r^{ap} is the distance between the friction force differential (dF_R) application point and the centre of the bearing, as illustrated in Figure 4:

$$r_i^{ap} = \frac{D_{pw}}{2} \pm \left(\bar{r}_i^2 + x_i^2\right)^{1/2} cos\left[\alpha_i \pm atan\left(\frac{x_i}{\bar{r}_i}\right)\right] \tag{5}$$

The sign of the second term in equation (5) must be positive for the outer ring (CP1 and CP4), and negative for the inner one (CP2 and CP3), while the sign inside the cosine will be positive for the contact diagonal 1(CP1 and CP3), and negative for the contact diagonal 2 (CP2 and CP4). Using cylindrical coordinates (ρ,θ) in equation (4) instead of cartesian coordinates (x,y) in Figure 4, the integration limits are defined and thus the computation process is simplified. The relation between cylindrical and cartesian coordinates is:

$$x_i = a_i \rho cos\theta \tag{6}$$

$$y_i = b_i \rho sin\theta \tag{7}$$

3. RESULTS AND DISCUSSION

When the ball rolls, a no-slip band exists in the contact ellipse [16], which divides the contact area into three different regions: the one in the centre is known as the backward slip region, whereas the other two, at both sides, are the foreward slip regions. In the backward region, the ball´s relative velocities with respect to the raceway have the opposite direction of the ball´s relative displacement, so shear stresses due to friction have the same direction as the relative movement. On the contrary, in the foreward regions friction forces act against this relative movement. Considering elastic micro-deformations at the contact surface, a no-slip region rather than a no-slip band will exist. Furthermore, and as it was expected, FE calculations show that the stick region is not only located between the backward and foreward regions, but also along the leading edge of the contact ellipse, as it can be observed in Figure 1b and Figure 5. As explained in the introduction section, the presence of this stick region contravenes the full sliding assumption made by the analytical models of Jones or Leblanc and Nelias, who computed shear stresses as the product of the pressure and the friction coefficient; obviously, in the stick region, shear stress will be equal or lower than that value. Nevertheless, full sliding hypothesis does not necessarily involve an overestimation of friction torque: depending on the extension and the location (backward or forward zone) of the stick region, the value of the friction torque can be higher or lower than the one calculated under full sliding assumption, so no clear tendency can be deducted without a more thorough study.

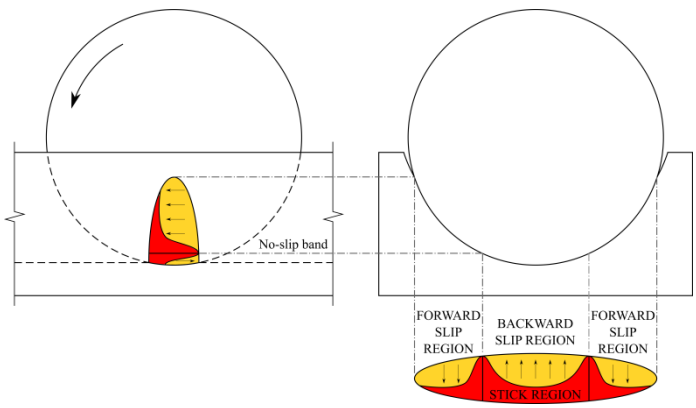

Figure 5. Contact ellipse regions in a ball rolling on a grooved track.

As a first step, and before comparing FE and analytical models, a sensitivity analysis was performed with the FE model in order to evaluate the effect of each parameter on the stick region of the contact ellipse.

3.1. Sensitivity analysis

The objective of this preliminary study is to set out the cases for the FE-analytical comparison presented in the next section. The parameters of the sensitivity analysis are the ball diameter (D_w), mean diameter of the bearing (D_{pw}), contact angles after loading (α), osculation ratio (s), friction coefficient (μ) and ball-raceway interferences (δ). First, a nominal design point using typical values of the parameters was defined; afterwards, each of the parameters was independently varied so that their influence could be qualitatively evaluated. The analyses were performed in an automated way taking advantage of the parametric nature of the model. Table 2 summarizes the maximum and minimum values for each parameter, where the interferences are expressed as a percentage over the static load-carrying capacity of the bearing for each case, which was calculated according to the analytical model developed previously by the authors [6].

	D_w	D_{pw}	α	s	μ	δ_1	δ_2
	[mm]	[mm]	[deg]	[-]	[-]	[%]	[%]
Nom	30	1000	45	0.95	0.100	50%	0%
Min	20	500	45	0.92	0.005	25%	0%
Max	40	2500	45	0.98	0.300	75%	0%

Table 2. Design space of the parametric study.

Stick regions only exist when the ball rolls, so the parametric study was carried out for the case of two contact points, i.e. one of the diagonals is unloaded in every case ($\delta_2 = 0$). The contact angle will affect the location of the contact ellipse (and thus the kinematics of the ball and the friction torque) but not the contact regions themselves. Consequently, a typical value of 45º was taken, as pointed out in Table 2, ensuring that no truncation of the ellipse will take place in any case. Although the truncation can be simulated through FE calculations, this effect is not considered in the analytical model; therefore, it has been avoided to allow a direct comparison between the models. Figure 6 shows the FE results of the contact status for all of the design points of the sensitivity analysis, where stick regions are represented in red and sliding zones in orange. From these results, the next conclusions arise:

- Ball diameter (D_w) and mean bearing diameter (D_{pw}) have no effect in the stick region in the studied design space. Thus, in slewing bearings, where the dimensions of the section are significantly smaller than the mean diameter ($D_w \ll D_{pw}$), none of these parameters will affect the stick region.
- The lower the osculation ratio (s), the more relevant will be the stick region. This effect is justified, because the contact ellipse grows with the conformity, moving away from the ideal condition of point contact with null relative velocity, and therefore making ball-raceway adhesion more unlikely.
- As it was predictable, sliding increases as friction coefficient (μ) decreases.
- Similarly to what happens with the conformity, ball-raceway adhesion becomes more difficult when the interference (δ) is increased due to the growth of the contact ellipse.

3.1. Comparison between analytical and Finite Element models

From the conclusions of the sensitivity analysis, two different case studies are compared in this section: Case A, where the values selected for parameters s, μ and δ favour the sliding, and Case B where the maximum area for the stick region is sought. The analytical model (which assumes full sliding) is expected to give accurate results for Case A; on the contrary, some discrepancies between analytical and FE results should be reported for Case B.

In order to extend the conclusions of the study to every load condition, three different subcases have been considered for both cases A and B: the first one with two contact points (allowing ball rolling) as in the sensitivity analysis; the second one for four equally loaded contact points, forcing ball spinning in all of the contacts; and finally the third one, which will be an intermediate case where four contact points will exist but one contact diagonal will be predominant over the other. Table 3 summarizes the parameters used for each analysis. Note that pick and valley values for conformity and friction coefficient do not match the ones in Table 2. This is because values in Table 3 correspond to typical values found in catalogues or obtained from experimental measurements [15] [19], while in the sensitivity analysis of Table 2 the design space was extended to evince the effect of each parameter.

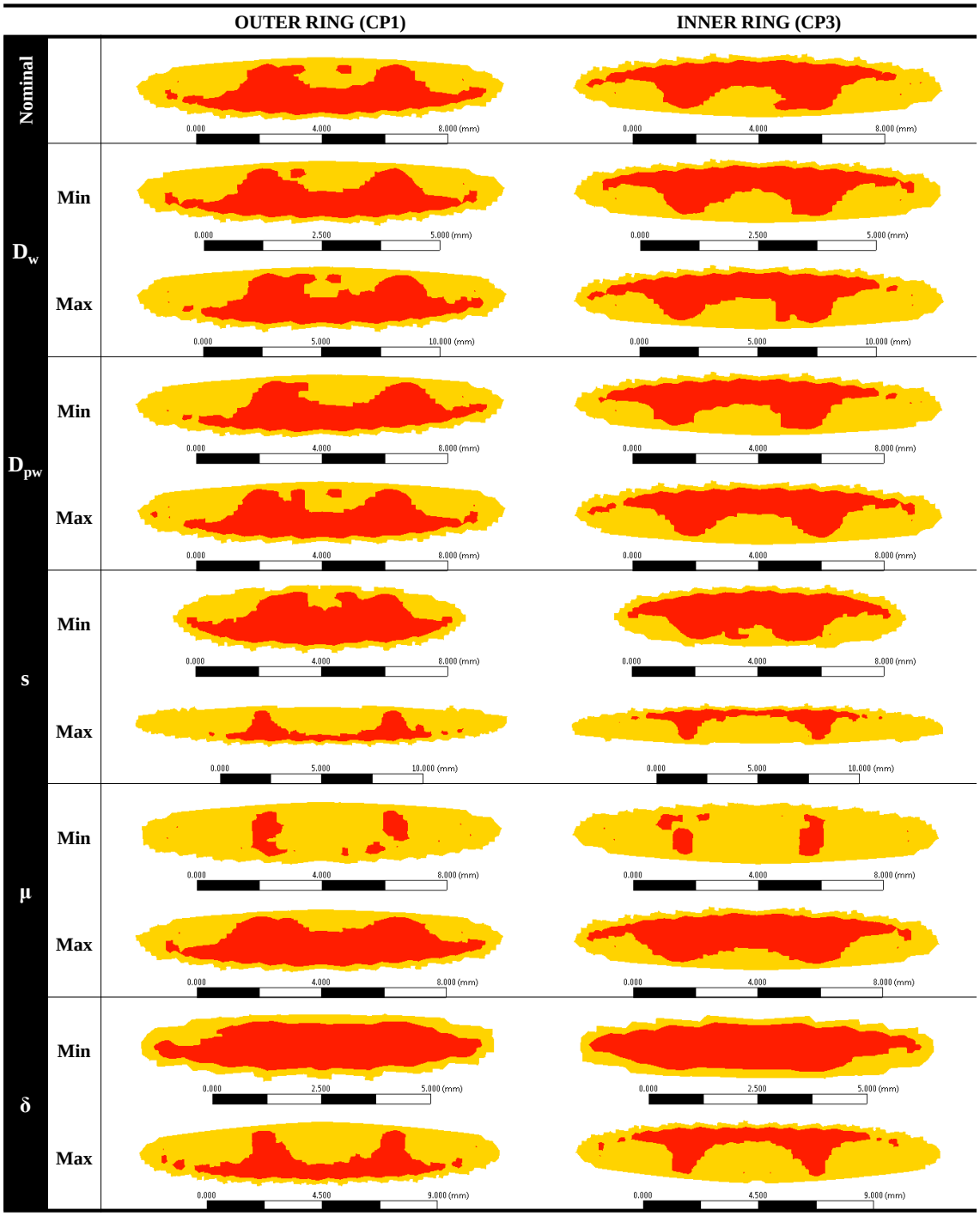

Figure 6. Stick region for studied cases.

	ID	D_w [mm]	D_{pw} [mm]	α [deg]	s [-]	μ [-]	δ_1 [%]	δ_2 [%]
	Nominal	30	1000	45	**0.95**	**0.10**	**50%**	**0%**
Case A Sliding favoured	**A1** (2CP)	30	1000	45	**0.96**	**0.09**	**75%**	**0%**
	A2 (4CP equally loaded)	30	1000	45	**0.96**	**0.09**	**75%**	**75%**
	A3 (4CP asymmetrically loaded)	30	1000	45	**0.96**	**0.09**	**75%**	**5%**
Case B Sticking favoured	**B1** (2CP)	30	1000	45	**0.94**	**0.13**	**25%**	**0%**
	B2 (4CP equally loaded)	30	1000	45	**0.94**	**0.13**	**25%**	**25%**
	B3 (4CP asymmetrically loaded)	30	1000	45	**0.94**	**0.13**	**25%**	**5%**

Table 3. Studied cases for analytical and FE models comparison.

The objective of the comparison between FE and analytical model is to highlight those cases where the predictive capabilities of the analytical model lack in accuracy. As the analytical model assumes full sliding in the ball-raceway contact, it will have certain limitations when computing shear stresses in the contact when the ball is rolling, which happens for two contact point cases (load case 1). The error will presumably be slight for limited stick regions (case A1), while a greater error is expected when the stick region prevails in the contact ellipse (case B1). On the other hand, in those cases where spinning occurs in the contacts (cases A2 and B2), the analytical model is foreseen to provide accurate results. These cases are studied to support the analytical model capabilities when full sliding occurs.

Figures 7 to 9 compare the analytical and FE results for contact shear stresses. They have been grouped according to the load condition, i.e. Figure 7 collects the cases with two contact points (cases A1 and B1), Figure 8 shows the results for equally-loaded four contact points (cases A1 and B2), and Figure 9 corresponds to intermediate cases (cases A3 and B3). Three plots are presented for each contact: in the upper plot the shear stresses calculated with the analytical model (LEB) are illustrated (the modulus with colours and the direction with arrows); the central plot corresponds to the FE model (FEM) results, with the same schema; finally, the lower plot illustrates the contact status of the FE model, with sliding region in orange and sticking region in red (remember that the analytical model assumes sliding in the whole contact ellipse).

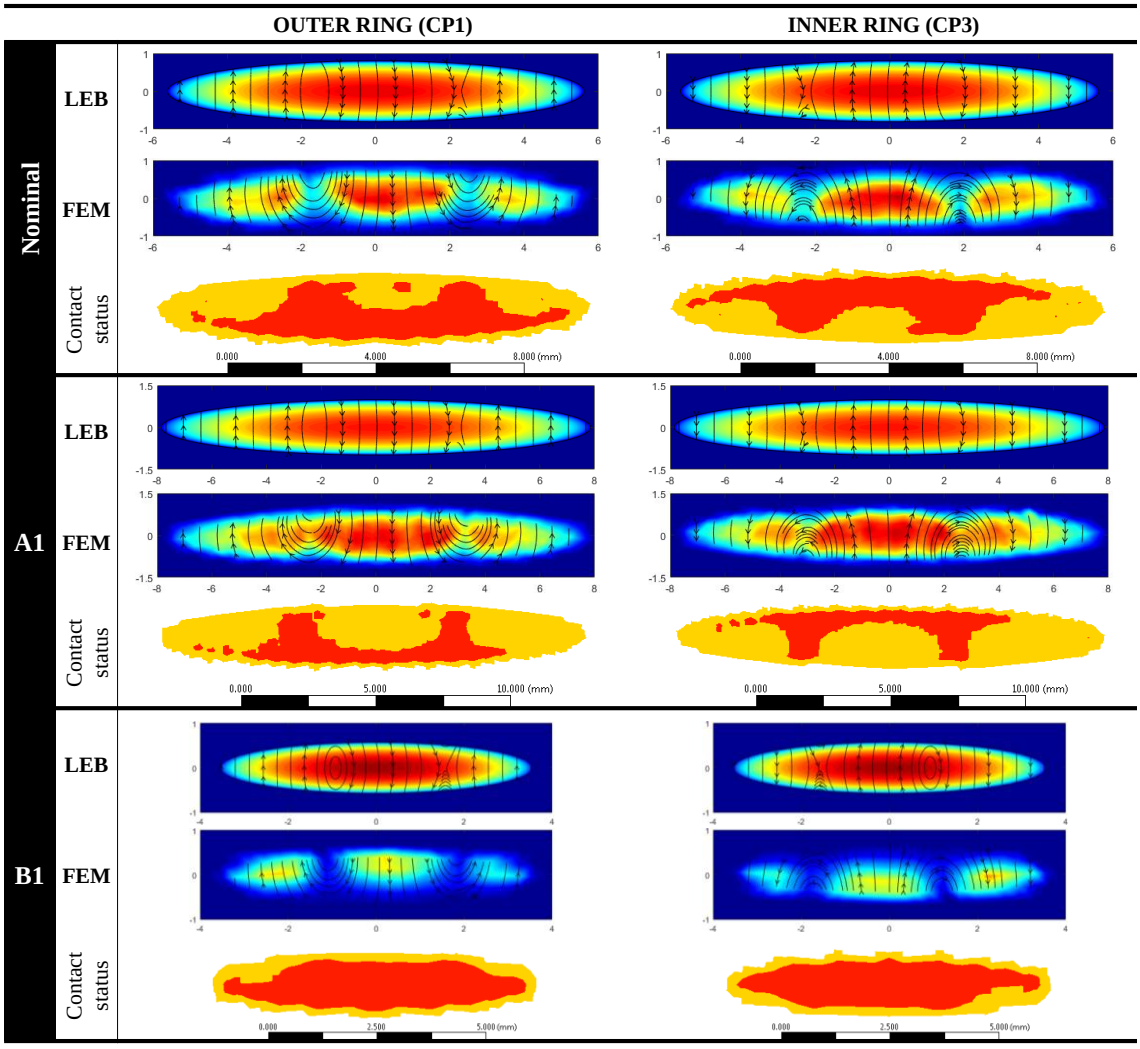

Figure 7. Leblanc model VS Finite element model for rolling cases.

In Figure 7, where ball rolling occurs due to the two contact point condition, differences between models can be appreciated. In the nominal case, shear stresses have the same modulus in the sliding regions while they differ in the stick zones. Changing s, μ and δ parameters to favour sliding (case A1), a better correlation is obtained. For larger stick regions (B1) shear stress field retrieved by the FE model is very different from the analytical one. Despite this error in the computation of the modulus, figures prove that the analytical model correctly predicts the direction of the shear stresses, i.e. the relative velocity field is well estimated. Another relevant aspect that FE results show is that the

adhesion of the leading edge moves backwards the vortex of the velocity field, instead of being placed in the major semi-axis of the ellipse as in the analytical model.

Figure 8, where ball spinning exists because the four contact points are equally loaded, shows a very good correlation between models, regardless of the s, μ and δ parameters. In both cases A2 and B2, the stick region in the spin pole is very small. Once again, as it happened for cases A1 and B1, these vortexes are moved backwards.

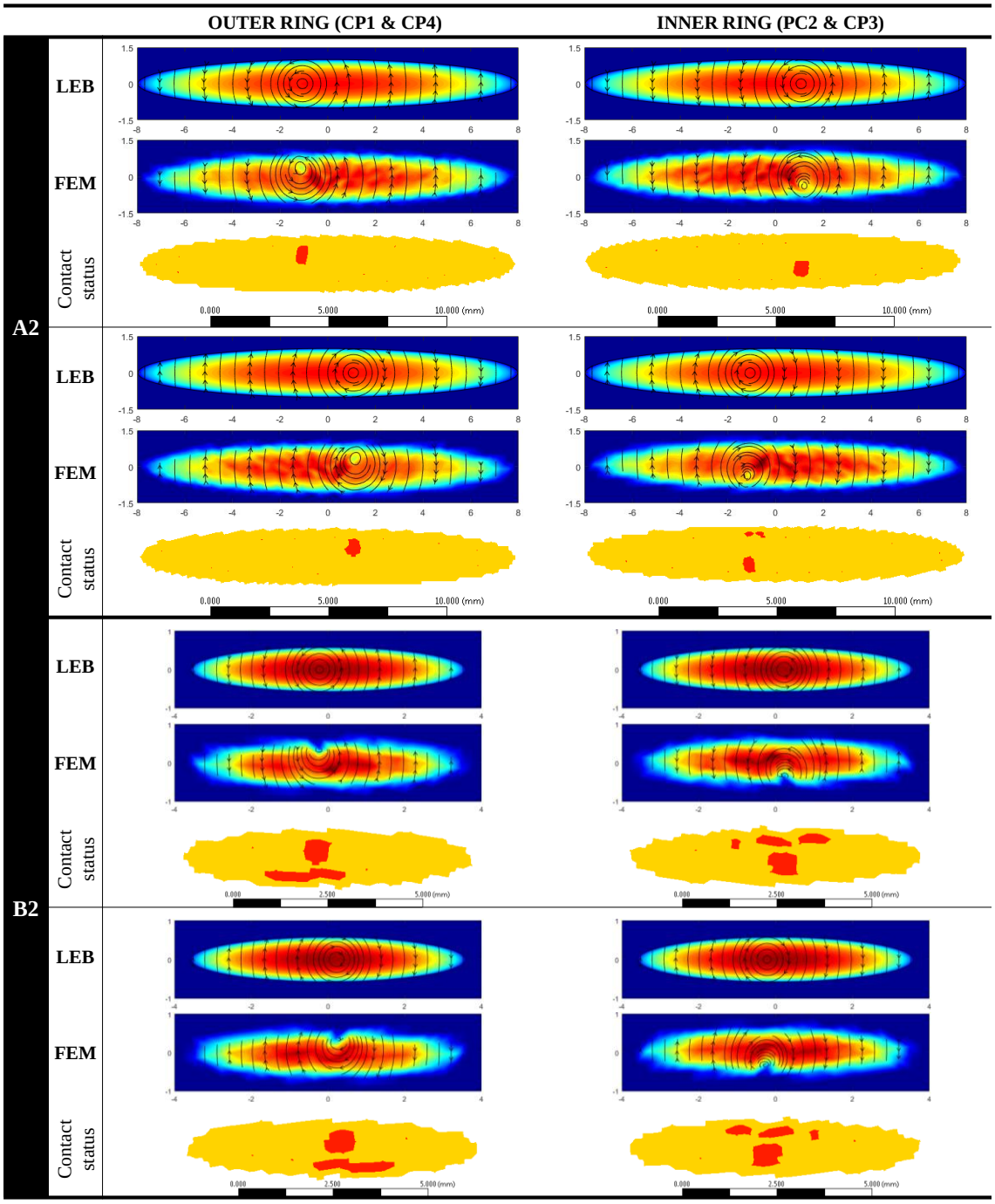

Figure 8. Leblanc model VS Finite element model for spinning cases.

Finally, Figure 9 shows two intermediate cases. In Case A3 one contact diagonal is significantly predominant over the other, so the ball rolls with respect to contact points 1 and 3 (see Figure 4), while full sliding occurs in points 2 and 4. Consequently, shear stress field in contact points 1 and 3 is very similar to case A1. On the contrary, in case B3 the most loaded contact diagonal is not so dominant, so the ball spins and shear stresses look similar to case B2.

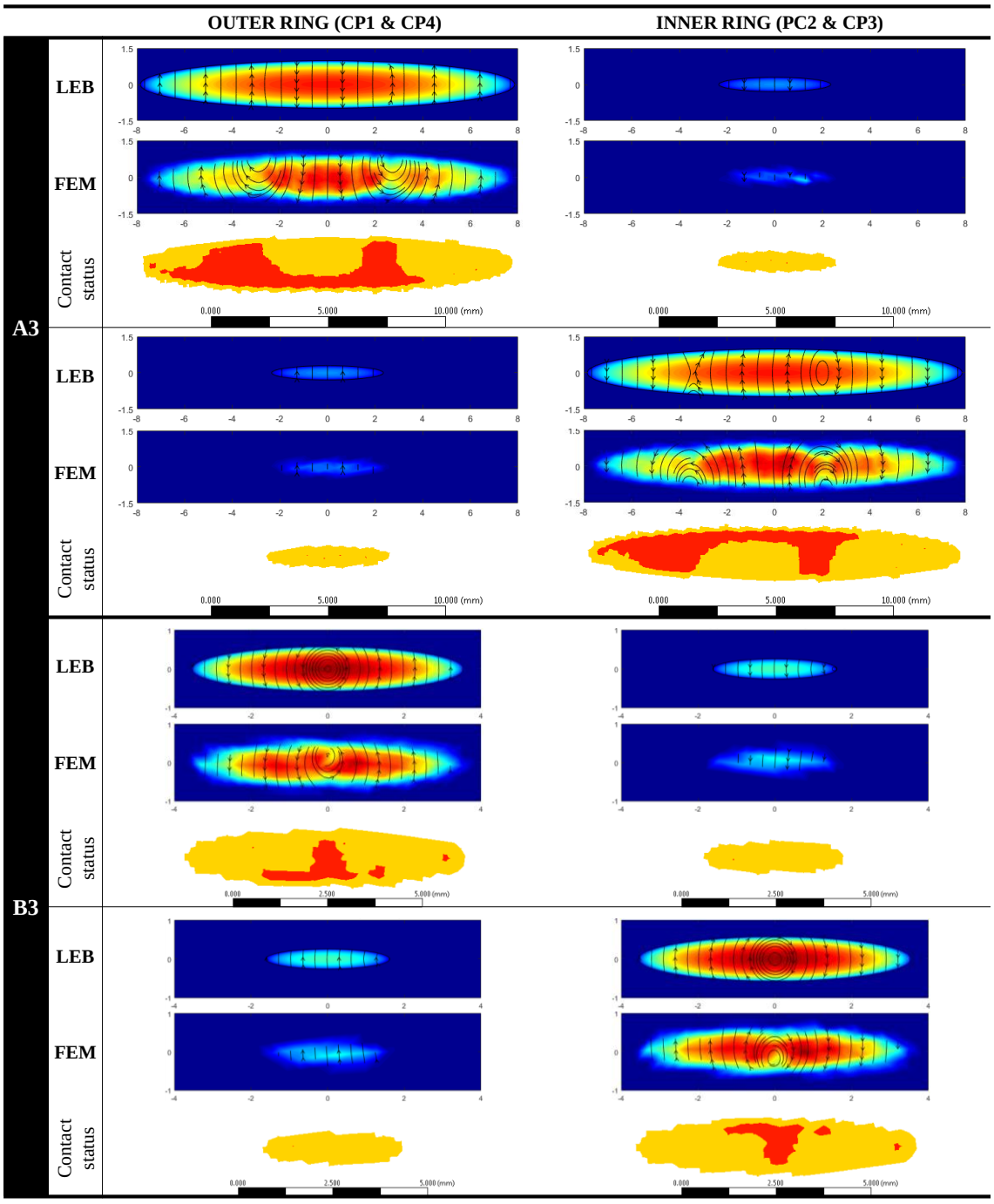

Figure 9. Leblanc model VS Finite element model for rolling or spinning plus sliding cases.

In order to quantitatively compare both models, Table 4 gives the results for friction torque and kinematics. The results confirm that for cases with full sliding (A2, B2 and B3), the analytical model proposed by Leblanc and Nelias provides very accurate friction torque values, giving an underestimation below 5%. Conversely, for cases with ball rolling (Nom, A1, A3 and B1), friction torque calculation is not so accurate, with errors in the ranging from -12% to +71% when comparing with the FE model. Not only the errors are large, but their values are also highly unpredictable. This fact can be clearly explained by studying extreme cases A1 and B1. In case A1, friction torque is underestimated by the analytical model, which means that in the FE model the backward region is more affected by the stick area than the forward region; as shear stresses in the backward region help the movement, if they decrease friction torque increases. On the other hand, in Case B1 stick region covers almost the whole contact ellipse, so shear stresses are below the analytical values, and thus the resulting friction torque is significantly lower. Notwithstanding this, kinematics are suitably calculated by the analytical model in all studied cases.

ID	BALL KINEMATICS (for ω_i = 1°/s)									FRICTION TORQUE			
	Movement nature		Ball angular speed (ω_B)				Ball angular speed angle (β)			Friction torque (M_f)			
	1-3	2-4	LEB	FEM	LEB *VS* FEM		LEB	FEM	LEB *VS* FEM	LEB	FEM	LEB *VS* FEM	
	[-]	[-]	[°/s]	[°/s]	[°/s]	[%]	[deg]	[deg]	[deg]	[N·m]	[N·m]	[N·m]	[%]
Nom	**Rolling**	-	33.0	32.9	0.1	0.4%	134.9	133.8	1.1	17.1	16.9	-1.0	**2%**
A1	**Rolling**	-	33.3	33.1	0.2	0.4%	134.8	133.9	0.9	64.7	73.4	-11.0	**-12%**
A2	**Spinning**	**Spinning**	43.4	42.8	0.6	1.4%	180.0	180.0	0.0	1165.4	1228.9	-63.6	**-5%**
A3	**Rolling**	**Sliding**	33.3	33.1	0.2	0.5%	136.3	135.9	0.4	138.9	158.3	-21.6	**-12%**
B1	**Rolling**	-	32.8	32.6	0.2	0.4%	135.0	133.8	1.2	2.9	1.7	0.7	**71%**
B2	**Spinning**	**Spinning**	45.5	45.1	0.4	1.0%	180.0	180.0	0.0	117.2	121.0	-3.8	**-3%**
B3	**Spinning**	**Sliding**	43.9	42.8	1.1	2.6%	176.9	175.8	1.1	57.5	59.4	-1.9	**-3%**

Table 4. Results for studied cases.

4. CONCLUSIONS

This manuscript studies the capabilities and limitations of the analytical model developed by Leblanc and Nelias for the analysis of four-point contact bearings, in particular for the calculation of friction torque in slewing bearings. For this purpose, a FE model was used to study the effect of different parameters in the stick region of the ball-raceway contact ellipse in order to compare its results with the analytical ones. From this work, the next conclusions are withdrawn:

- In cases where full sliding occurs, the analytical model proved to be a reliable and cost effective tool. Thus, it can be satisfactorily used when the ball is spinning, or when the stick region is negligible if it is rolling.
- When the ball rolls, analytical and FE friction torque results may significantly differ because shear stresses are poorly estimated by the analytical model, as observed in cases A1, A3 and B1 of this work.
- The stick zone can affect the backward and/or the foreward regions. Depending on the area covered by the stick zone in each of the regions, the analytical model will be conservative or not conservative in friction torque calculation in comparison with the FE model.
- If the stick region involves most of the contact ellipse and the ball is rolling, the analytical model overestimates friction torque. As an illustrative example, for case B1 of this work, friction torque is 71% higher for the analytical model than for the FE model.
- When the stick region affects only a small part of the contact ellipse and the ball is rolling, the analytical model underestimates friction torque in comparison with the FE model. The reason is that, for reduced stick zones, it is the backward region (where shear stress helps rolling movement) which is more affected by no-slip zones in the FE model. For instance, in case A1 the friction torque given by the analytical model was found to be 12% smaller than the FE result.

In the light of these particular conclusions, the following general conclusions have been deducted:

- In slewing bearings for orientation purposes, where balls mainly work with two contact points because of the large tilting moments, the load rate has a significant influence on the stick region. For light loads, the extension of the stick region covers most of the contact ellipse, and thus the analytical model proposed by Leblanc and Nelias overestimates the friction torque. Otherwise, for heavy loads, the analytical model underestimates it according to FE results. The torque actuation systems of the orientation systems must be dimensioned for ultimate loads, ergo using the analytical model may lead to undersized systems.
- Conformity ratio and friction coefficient also proved to have an important influence on the stick region. A model capable of suitably modelling stick regions would be decisive to determine the optimum values for these design parameters.
- For the sake of accuracy, more advanced formulations would be needed for the analytical modelling of the contact mechanics for applications under large tilting moments. The new analytical model should consider stick regions, as well as the micro-deformations in the contact ellipses. The authors will deal with this challenge in future work.

- Leblanc's analytical model has proved to determine the kinematics of the bearing quite accurately in any case, since these outputs do not seem to be significantly affected by the stick regions. Therefore, the authors think that it can be used to reliably predict the kinematics of slewing bearings in any application.

For the conclusions above, the FE model is presented as the reference when evaluating the accuracy of the analytical model. From the comparison, it can be seen that both models provide very similar results when full sliding occurs, supporting their predictive capacity in terms of friction torque calculation under such conditions. As the analytical model does not consider the effect of the stick in the contact ellipse, discrepancies have been detected when this effect is present. In this manuscript, the FE model is proved to represent the stick zones of the contact and the results are logical and coherent. Nevertheless, despite the high accuracy expected from such a detailed FE model, further work will be done in order to obtain more accurate contact results. In this sense, submodelling techniques will be used, allowing a much finer local mesh with an affordable computational cost. Furthermore, this refined model will allow the validation of the FE model presented in this manuscript. As a final validation, experimental tests are planned; for this purpose, the friction torque will be measured in a test bench for different bearings.

ACKNOWLEDGEMENTS

This paper is a result of the close collaboration that the authors maintain with the company Iraundi S.A. This work was supported by the Ministry of Economy and Competitiveness of Spain [project number DPI2013-41091-R] and the University of the Basque Country (UPV/EHU) [project number UFI 11/29].

REFERENCES

[1] S. Zupan, I. Prebil, Carrying angle and carrying capacity of a large single row ball bearing as a function of geometry parameters of the rolling contact and the supporting structure stiffness, Mech. Mach. Theory. 36 (2001) 1087–1103. doi:10.1016/S0094-114X(01)00044-1.

[2] S. Zupan, I. Prebil, R. Kunc, M. Češarek, Internal load distribution in large sized axial rolling bearing mounted on elastic structures, VDI. Ber. 1706 (2002) 639–656.

[3] J.I. Amasorrain, X. Sagartzazu, J. Damián, Load distribution in a four contact-point slewing bearing, Mech. Mach. Theory. 38 (2003) 479–496. doi:10.1016/S0094-114X(03)00003-X.

[4] J. Aguirrebeitia, J. Plaza, M. Abasolo, J. Vallejo, General static load-carrying capacity of four-contact-point slewing bearings for wind turbine generator actuation systems, Wind Energy. 16 (2013) 759–774. doi:10.1002/we.1530.

[5] J. Aguirrebeitia, M. Abasolo, R. Avilés, I. Fernández de Bustos, General static load-carrying capacity for the design and selection of four contact point slewing bearings: Finite element calculations and theoretical model validation, Finite Elem. Anal. Des. 55 (2012) 23–30. doi:10.1016/j.finel.2012.02.002.

[6] J. Aguirrebeitia, J. Plaza, M. Abasolo, J. Vallejo, Effect of the preload in the general static load-carrying capacity of four-contact-point slewing bearings for wind turbine generators: theoretical model and finite element calculations, Wind Energy. 17 (2014) 1605–1621. doi:10.1002/we.1656.

[7] M. Olave, X. Sagartzazu, J. Damian, A. Serna, Design of Four Contact-Point Slewing Bearing With a New Load Distribution Procedure to Account for Structural Stiffness, J. Mech. Des. 132 (2010) 21006. doi:10.1115/1.4000834.

[8] J. Plaza, M. Abasolo, I. Coria, J. Aguirrebeitia, I. Fernández de Bustos, A new finite element approach for the analysis of slewing bearings in wind turbine generators using superelement techniques, Meccanica. 50 (2015) 1623–1633. doi:10.1007/s11012-015-0110-7.

[9] S. Aithal, N. Siva Prasad, M. Shunmugam, P. Chellapandi, Effect of manufacturing errors on load distribution in large diameter slewing bearings of fast breeder reactor rotatable plugs, Proc. Inst. Mech. Eng. Part C J. Mech. Eng. Sci. 0 (2015) 1–12. doi:10.1177/0954406215579947.

[10] I. Heras, J. Aguirrebeitia, M. Abasolo, Friction torque in four contact point slewing bearings: Effect of manufacturing errors and ring stiffness, Mech. Mach. Theory. 112 (2017) 145–154. doi:10.1016/j.mechmachtheory.2017.02.009.

[11] A.B. Jones, Ball Motion and Sliding Friction in Ball Bearings, J. Basic Eng. 81 (1959) 1–12.

[12] A. Leblanc, D. Nelias, Ball Motion and Sliding Friction in a Four-Contact-Point Ball Bearing, J. Tribol. 129 (2007) 801–808. doi:10.1115/1.2768079.

[13] A. Leblanc, D. Nelias, Analysis of Ball Bearings with 2, 3 or 4 Contact Points, Tribol. Trans. 51 (2008) 372–380. doi:10.1080/10402000801888887.

[14] S. Lacroix, D. Nelias, A. Leblanc, Four-Point Contact Ball Bearing Model With Deformable Rings, J. Tribol. 135 (2013) 1–8. doi:10.1115/1.4024103.

[15] A. Joshi, B. Kachhia, H. Kikkari, M. Sridhar, D. Nelias, Running Torque of Slow Speed Two-Point and Four-Point Contact Bearings, Lubricants. 3 (2015) 181–196. doi:10.3390/lubricants3020181.

[16] B. Bhushan, Friction, in: Princ. Appl. Tribol., John Wiley & Sons, Ltd, 2013: pp. 321–401. doi:10.1002/9781118403020.ch6.
[17] J. Aguirrebeitia, M. Abasolo, J. Plaza, I. Heras, FEM model for friction moment calculations in ball-raceway contacts for applications in four contact point slewing bearings, in: 14th World Congr. Mech. Mach. Sci. 25-30 Oct., Taipei, Taiwan, 2015. doi:10.6567/IFToMM.14TH.WC.OS18.018.
[18] J.J. Kalker, Three-Dimensional Elastic Bodies in Rolling Contac, Springer Netherlands, 1990. doi:10.1007/978-94-015-7889-9.
[19] D. Gonçalves, S. Pinho, B. Graça, A. V. Campos, J.H.O. Seabra, Friction torque in thrust ball bearings lubricated with polymer greases of different thickener content, Tribol. Int. 96 (2016) 87–96. doi:10.1016/j.triboint.2015.12.017.